JOURNAL OF MATERIALS SCIENCE 28 (1993) 4078–4084

Fracture behaviour and morphology of PC/ABS blends

S. SEIDLER, W. GRELLMANN
Department of Materials Science, Martin-Luther-University Halle-Wittenberg, 06247, Merseburg, Germany

The toughness behaviour of polycarbonate (PC)/acrylnitrile-butadiene-styrene (ABS) blends under dynamical loading (1 $m s^{-1}$) based on the *J*-integral concept was studied. For this the multiple specimen *R*-curve method was used. A special experimental technique of a stop block method was developed. It was shown that the materials exhibit a very different toughness behaviour depending on temperature and ABS content. The reasons for this material behaviour are discussed with the help of scanning and transmission electron microscopical (SEM and TEM) investigation methods. It can be shown that a combination of fracture mechanics and electron microscopy allows a toughness optimization to be made on the basis of quantitative morphology–toughness correlations.

1. Introduction

In technical application, toughness is the most often optimized property of polymer blends. For these materials, the improvement of toughness behaviour at low temperatures (up to $T = -30\,°C$) is of special interest. The basic requirement for optimized toughness properties is a material with high energy consumption.

The application of fracture mechanical investigation methods in conjunction with the evaluation concepts of yield fracture mechanics, makes it possible to quantify crack initiation, crack-growth behaviour and energy dissipative processes occurring during stable crack growth [1–3].

The instrumented notched bar impact test was used as a testing method [4], because the toughness characterization of polymers is generally accomplished by means of conventional impact tests. Therefore, on the basis of an energetic interpretation of deformation and fracture behaviour in conjunction with investigations on morphology, a theoretically based toughness optimization is possible [5, 6]. The fracture behaviour of polymer blends is characterized by dominant stable crack growth. In this case, the load–deflection diagrams exhibit crack propagation energies after maximum impact load. Fig. 1 shows selected load–deflection diagrams of PC/ABS blends. From these diagrams it is evident that:

1. in PC, the dominant crack-growth mechanism is unstable crack propagation. Fracture surface analysis also proves that stable crack growth now occurs;
2. crack propagation is, however, stable in the blends, which can be shown by means of the large crack propagation energies, A_R
3. in ABS, crack propagation is both unstable and stable, but stable crack growth is the dominant mechanism.

From this load–deflection behaviour it may be deduced that a uniform toughness characterization of these blends depending on concentration is not possible, if one considers previous knowledge of the use of different fracture mechanical concepts. The toughness characterization of PC must be carried out with fracture mechanics values which characterize material resistance, as opposed to unstable crack growth, because of the dominant unstable crack-growth mechanism (for instance *J*-integral, the evaluation method of Sumpter and Turner [7]). The toughness characterization of the blends and ABS must be accomplished using crack resistance (*R*) curves.

2. Materials and methods

For the investigations, the different PC/ABS blends of Bayer AG Leverkusen were used: T 45 MN with 45% PC, T 65 MN with 60% PC, T 85 MN with 70% PC. The specimens were produced by compounding on a double-screw extruder and then moulding.

Single-edge notched (SENB) specimens were used for this study. The dimensions of the specimens were: length $L = 80$ mm, width $W = 10$ mm and thickness $B = 4$ mm. The specimens were notched with a razor blade. The notch-tip radius was 0.2 μm and the notch depth, a, was 4.5 mm, i.e. $a/W = 0.45$. The support span, s, was 40 mm, i.e. $s/W = 4$, and the pendulum hammer speed $v_H = 1.5\ m s^{-1}$. In principle, crack resistance curves are a function of the loading parameter (*J*-integral, crack opening displacement) on the stable crack growth, Δa. These curves can be determined by the loading of specimens such that stable cracks with different lengths, Δa, are formed, Load–deflection diagrams are recorded parallel to this.

Stable crack growth, Δa, is quantified on the fracture surface by light microscopy. The fracture surfaces are produced by breaking the specimens at liquid nitrogen temperature and high pendulum hammer

0022–2461

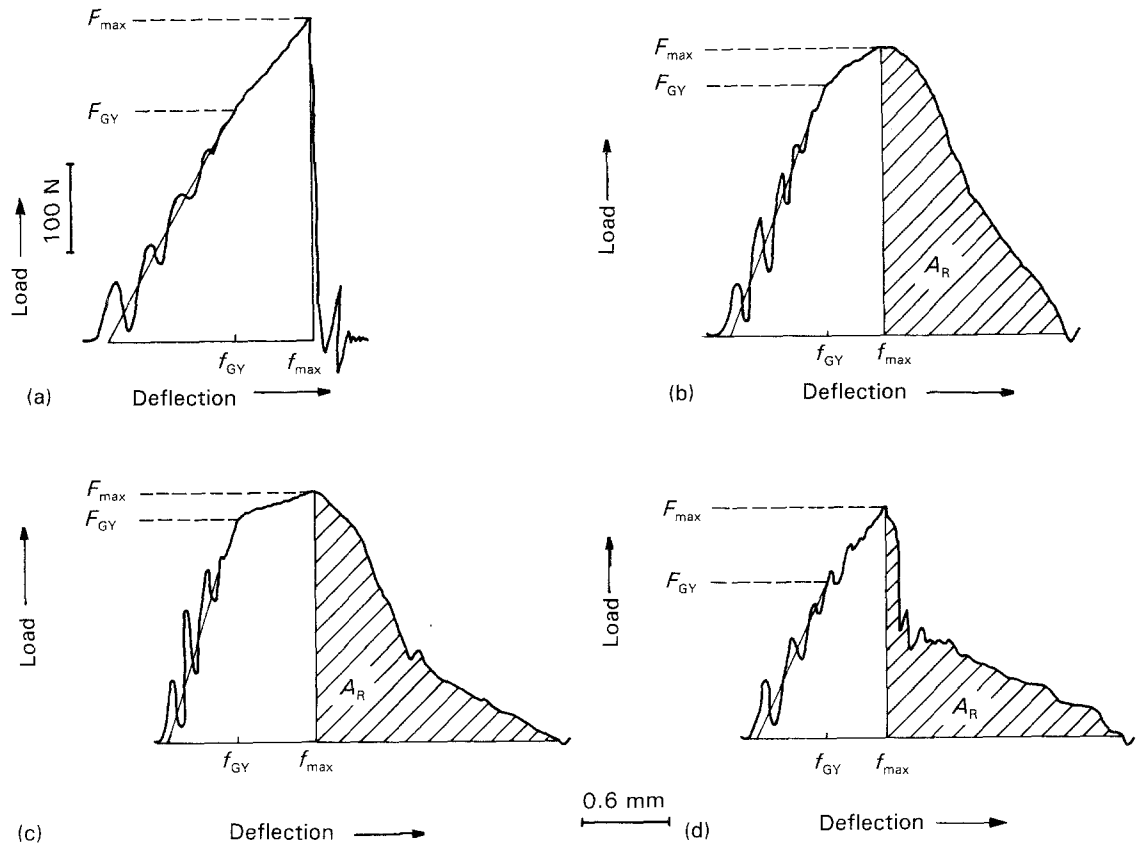

Figure 1 Characteristic load (F)–deflection (f) diagrams of (a) PC, (b) PC/ABS = 70/30; (c) PC/ABS = 30/70; (d) ABS and selected PC/ABS blends.

speed. The measurements cover total crack growth [8].

The value of J for each specimen was determined from the area under its load–deflection curve (Equation 1)

$$J = \left[\eta_{el}\frac{A_{el}}{B(W-a)} + \eta_{pl}\frac{A_{pl}}{B(W-a)}\right]\left[1 - \frac{(0.75\eta_{el}-1)\Delta a}{(W-a)}\right] \quad (1)$$

$$\eta_{el} = \frac{2F_{GY}s^2(W-a)}{f_{GY}E_d BW^3} f^2(a/W)(1-\nu^2) \quad (2)$$

$$\eta_{pl} = 2 - \frac{(1-a/W)(0.892-4.476a/W)}{1.125+0.892(a/W)-2.238(a/W)^2} \quad (3)$$

where $A_{el,pl}$ is the elastic (plastic) share of the total deformation energy up to maximum impact load, F_{GY}, f_{GY} the load (deflection), corresponding to the transition from elastic to elastic–plastic material behaviour, $f(a/W)$ the function of crack length to width for the three point bend specimen, ν is Poisson's ratio, and E_d is the dynamical Young's modulus.

There are two reasons for selecting Equation 1. On the one hand, an exact determination of the J-integral value requires knowledge of stable crack growth during the experiment and, on the other hand, the J values determined from Equation 1 agree best with the J values which are determined by the iterative solving method proposed in by Zerbst and Will [9]. Another advantage of Equation 1 is that the restriction of Δa which is contained in the standards [10–12] for the determination of valid J-integral values will be irrelevant.

The crack resistance curve of yield fracture mechanics includes the processes of crack-tip blunting characterized by the blunting line

$$J = 2R_e\,\Delta a \quad (4)$$

crack initiation, determined as the technical crack initiation value from the point of intersection of a parallel line offset to the blunting line at 0.2 mm crack growth, and by the R curve. The slope of the R curve is a value for materials resistance against stable crack growth, and it can be quantified by the Tearing modulus, T_J

$$T_J = \frac{dJ}{d(\Delta a)}\frac{E}{R_e^2} \quad (5)$$

For the measurements, a Charpy impact tester PSW 0.4 of 4 J work capacity was used and load (F)–deflection (f) diagrams were recorded. Semiconductor strain gauges were used to record the impact load. The deflection was recorded with the help of a photo-optical system. A special experimental technique is necessary for the recording of dynamic crack resistance curves, which makes it possible to supply different energy values to the specimens. For this, different methods are known, but the most important is the stop block technique [13]. Here, different amounts of stable crack growth are produced by varying the limitation of deflection. This limitation can be accomplished by hardened steel deflection stops [14] or by catching the pendulum hammer, as shown in Fig. 2.

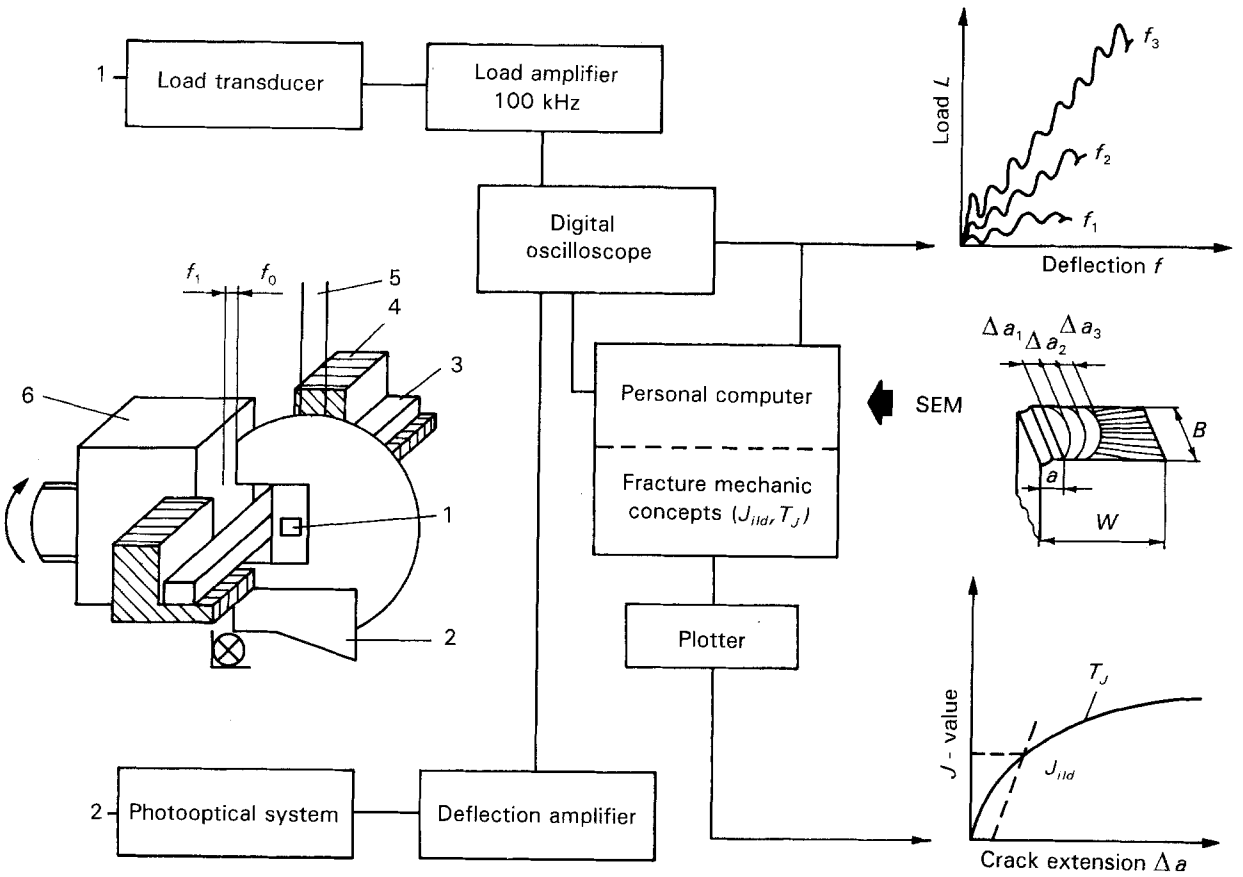

Figure 2 Fracture mechanics workplace of the computer-assisted instrumented Charpy impact test system with stop block arrangement. 1, semiconductor strain gauges; 2, optical deflection transducer; 3, specimen; 4, support; 5, pendulum; 6, hardened-steel deflection stop.

3. Results and discussion

The purpose of the fracture mechanical investigations was to quantify the influence of concentration and temperature on the crack resistance behaviour of the materials chosen. The results of the investigations at room temperature are shown in Fig. 3. The $J - \Delta a$ values were fitted by a power law as prescribed in the standards [10–12]. It can be shown that the crack initiation behaviour is not strongly influenced by the concentration, but it is remarkable that the T_J value of T 65 MN is very small in comparison to that of the other materials. The reasons for this material behaviour were first investigated by a fracture surface analysis using SEM. From Fig. 4 it becomes clear that a strong formation of cavities occurs during loading in the T 85 MN. From the heterogenity and the multi-ply nature of the fracture surface, it can be concluded that there are many local crack initiation sites which are the cause of the increase of the local plastic matrix deformation of the PC. There is a regional matrix fibrillation, and these regions are distributed regularly on the fracture surface, but they exist independently of each other (Fig. 5). In the T 45 MN, a matrix fibrillation was found only in the transition of the initial crack, a, to the fracture surface (Fig. 6a). In the crack growth direction, only single fibrils appear (Fig. 6b). The fracture surface is also porous and multi-ply.

In contrast, the fracture surface of T 65 MN exhibits a smooth appearance (Fig. 7) and no fibrils. We have shown elsewhere [13, 15] that the tearing modulus, T_J, is an extremely sensitive indicator of changes in morphology. Already with the aid of the fracture surface observations it becomes clear that the T 65 MN which has the lowest T_J value also has the lowest share of the provable energy dissipative processes. The reasons for this material behaviour will be discussed in connection with the results of the investigations of the influence of temperature on crack initiation behaviour. Fig. 8 shows the influence of the temperature on the recorded load–deflection diagrams. The F–f behaviour was nearly the same for all products investigated. With increasing temperature of the maximum impact load, F_{Max}, maximum deflection, f_{Max}, and A_{pl} increase, crack propagation energies reach temperatures $\geqslant -70\,^{\circ}C$, and they are nearly constant up to $T = -45\,^{\circ}C$. If the temperature increases further, a strong increase in all measured values can be observed. At temperatures $\geqslant -30\,^{\circ}C$, stable crack growth dominates. At room temperature, no specimen fracture occurs under the experimental conditions chosen.

Fig. 9 shows the dynamic R curves of the Bayblends which depend on concentration and temperature. The fracture mechanic values which are determined from these R curves are summarized in Table I. With increasing temperature, the crack initiation values, J_{ild}, increase for all products. The result is marked by obviously lower J_{ild} values than the other products. This tendency reverses with increasing temperature.

The T_J values show a similar behaviour with increasing temperature, but the influence of temperature on this value is considerably higher than on the J_{ild}

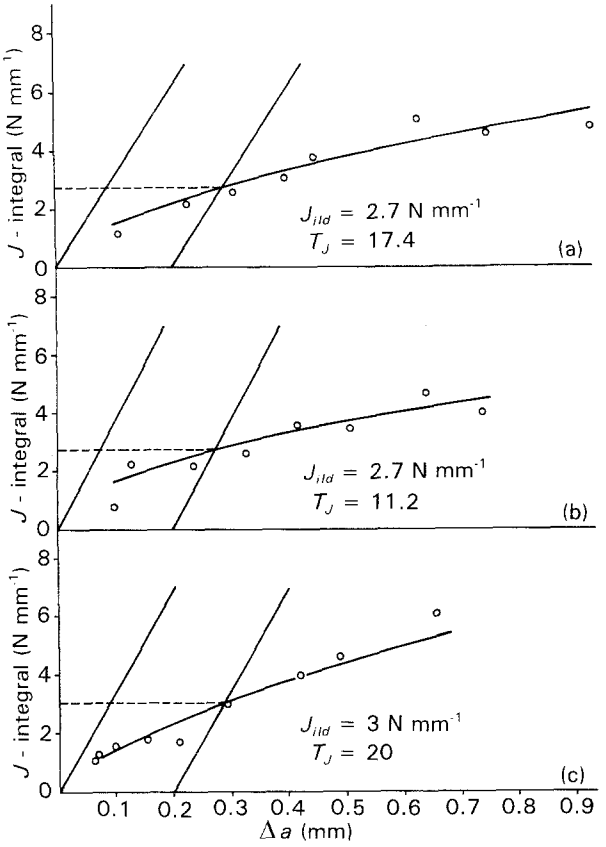

Figure 3 Dynamical crack resistance curves of the Bayblends ($V_H = 1\ m\ s^{-1}$). (a) T45 MN, (b) T65 MN, (c) T85 MN.

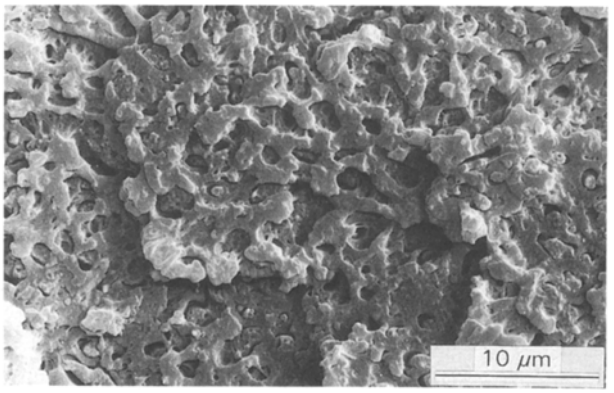

Figure 4 SEM observation of T 85 MN.

values, especially for the products T 45 MN and T 65 MN. It is noteworthy that the T 85 MN material shows a higher resistance to stable crack growth at all temperatures.

In addition to the SEM observations, TEM observations were carried out to discover the causes of toughness behaviour in the blends. The TEM observations were made on OsO_4 contrasted ultra-thin cuts, and parallel to that a quantitative morphology analysis was accomplished. The ABS was found, in general, to be a "porous" structure (Fig. 10).

The light elements of ABS can be assigned to the acrylonitrile. The ABS structure is homogeneous; there are no differences in phase concentration. The interface structure PC/ABS points to a good phase coupling.

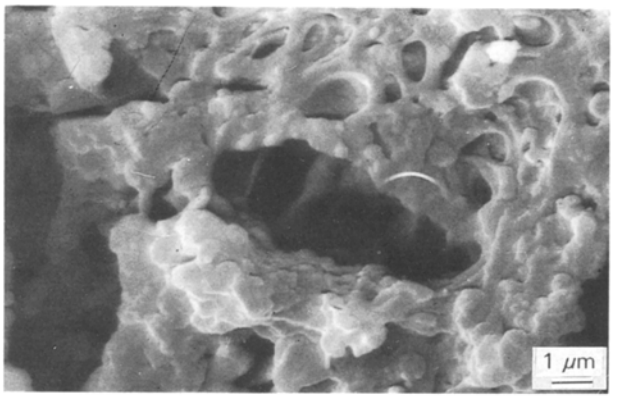

Figure 5 Streched matrix sphere in T 85 MN.

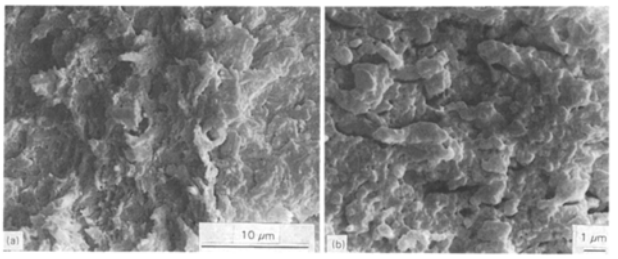

Figure 6 Fracture surface of T 45 MN: (a) transition sphere, initial crack-fracture surface, (b) centre of fracture surface.

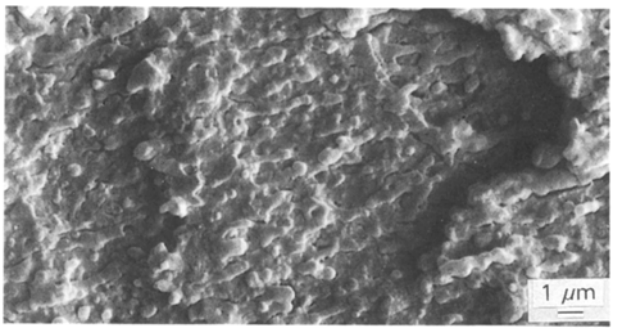

Figure 7 SEM observation of T 65 MN.

In increasing the toughness of the polymer, several phase systems generally occur about the initiation of energy dissipative processes, such as formation of crazes or shear bends. For the initiation of such processes, optimum particle sizes, and especially optimum particle distances, of the inserted component are necessary. These particle sizes and distances depend on the kind of components employed and on their concentration.

As a decision criterion for the fracture behaviour of such systems, Wu [16], specifies a matrix-specific critical particle distance. According to Wu [16], a system reacts in a brittle manner if this critical distance is exceeded, and in a ductile manner if the distance is not reached. For impact-modified polyamide, this critical partical distance is 304 nm. For blends with PC matrix material, such results are unknown thus far. For this material, it is clear that the critical particle distance is not reached, because the materials exhibit a ductile fracture behaviour under the experimental conditions chosen. For toughness of the Bayblends

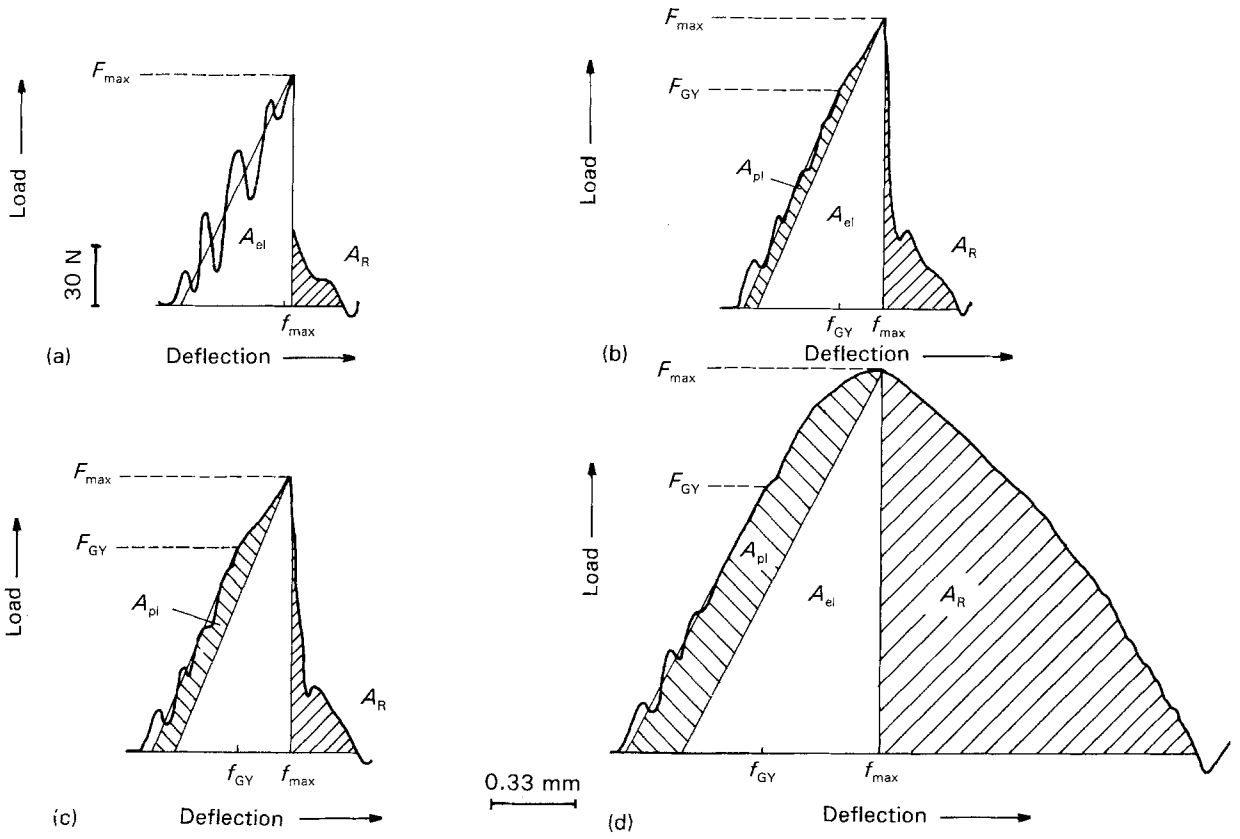

Figure 8 Load–deflection behaviour of T 85 MN which depends on test temperature: (a) − 100 °C, (b) − 70 °C, (c) − 50 °C, (d) − 30 °C.

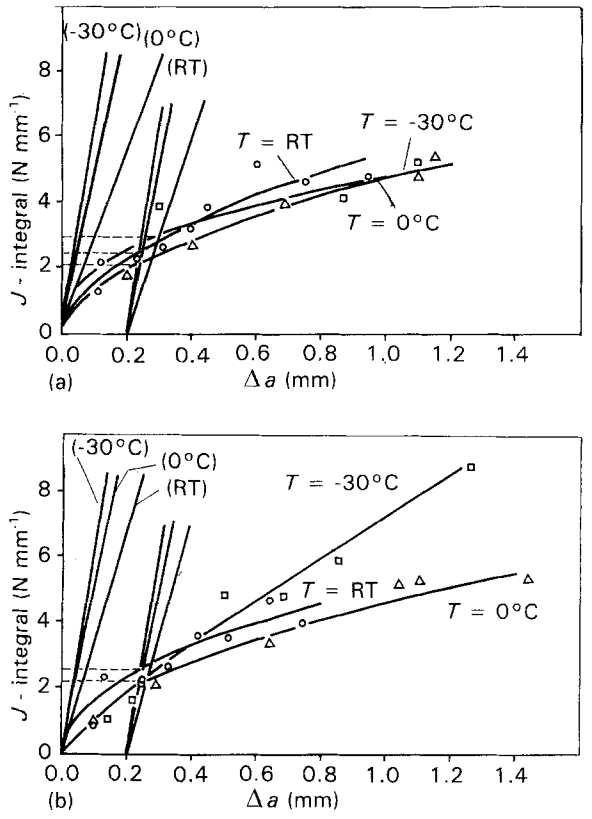

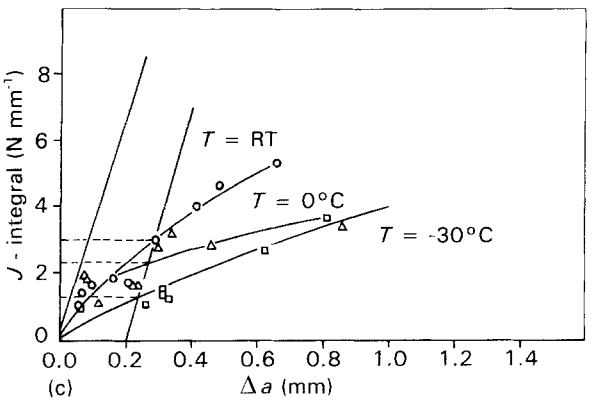

Figure 9 J_R curves of the Bayblends which depend on concentration and temperature. (a) T 45 MN, (b) T 65 MN, (c) T 85 MN.

particle size, particle direction and particle distribution are therefore the important factors.

Fig. 11a–c show selected TEM observations of T 85 MN (Fig. 11a), T 65 MN (Fig. 11b) and T 45 MN (Fig. 11c). It becomes clear that with increasing ABS content, the orientation of the phases with respect to each other changes.

The ABS phase has a relatively fine distribution, and the particles are nearly spherical in the T 85 MN. In contrast, the ABS particles in the T 65 MN and T 45 MN are flat and have the form of lancets. Table II shows the results of quantitative morphological analysis. The analysis of morphology shows that both the average and maximum particle size and the distribution breadth of T 65 MN are larger than those of other materials. T 85 MN and T 45 MN show comparable morphology parameters. The inclusion of the results of the morphology investigations in the discussion of the fracture mechanical values yields the following results.

The crack initiation behaviour of the blends is determined by the ABS content at $T = -30\,°C$. In contrast, the Tearing modulus is influenced by the direction of the ABS particles.

TABLE I Fracture mechanical values of the Bayblends which depend on temperature and concentration

Bay-blend	$T = -30\,^{\circ}C$		$T = 0\,^{\circ}C$		$T = RT$	
	J_{ild} ($N\,mm^{-1}$)	T_J	J_{ild} ($N\,mm^{-1}$)	T_J	J_{ild} ($N\,mm^{-1}$)	T_J
T45MN	2.1	3.6	2.4	4.6	2.7	17.4
T65MN	2.2	5.7	2.2	6.2	2.7	11.2
T85MN	1.2	14.9	2.3	12.0	3.0	20.0

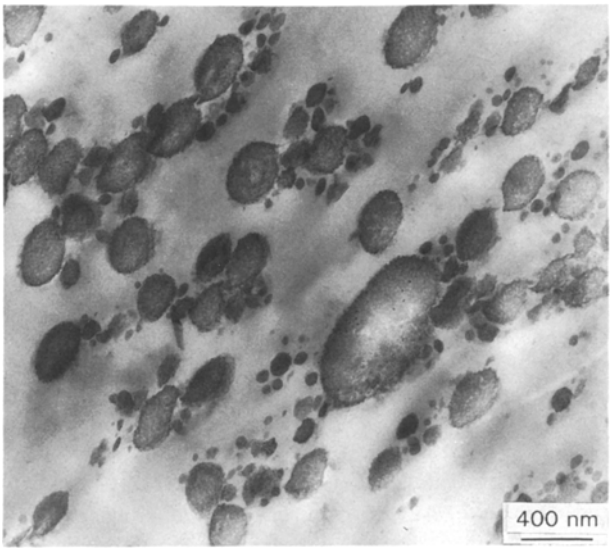

Figure 10 An ABS particle in T 65 MN.

T 85 MN shows the highest T_J values at all temperatures. From this it follows that a fine and disperse distribution of spherical ABS particles also effects an optimum material resistance against stable crack growth at low temperatures. The fact that the ABS particles are structures like a string of pearls is the main reason for the comparatively low T_J values of T 65 MN and T 45 MN at low temperatures. A homogeneous and disperse particle distribution is necessary for the initiation of energy dissipative processes which begin at the inserted ABS particles, because only under these conditions can the particles initiate crazing or shear bending. The existing phase direction in the T 65 MN and T 45 MN with the orientation of ABS in the blends influences the crack resistance behaviour negatively, especially at low temperatures.

At room temperature, the differences are comparatively small for the crack initiation values J_{ild}, and the T_J values of T 85 MN and T 45 MN are also nearly the same. A very small T_J value was found for the T 65 MN in comparison with the other products at room temperature. Here the negative effect of breadth particle-size distribution with a comparatively large number of large particles becomes clear.

The values J_{ild} and T_J enable quantification of the crack initiation and crack-growth behaviour, but it is not possible to quantify the energy dissipative processes occurring during stable crack growth with these values.

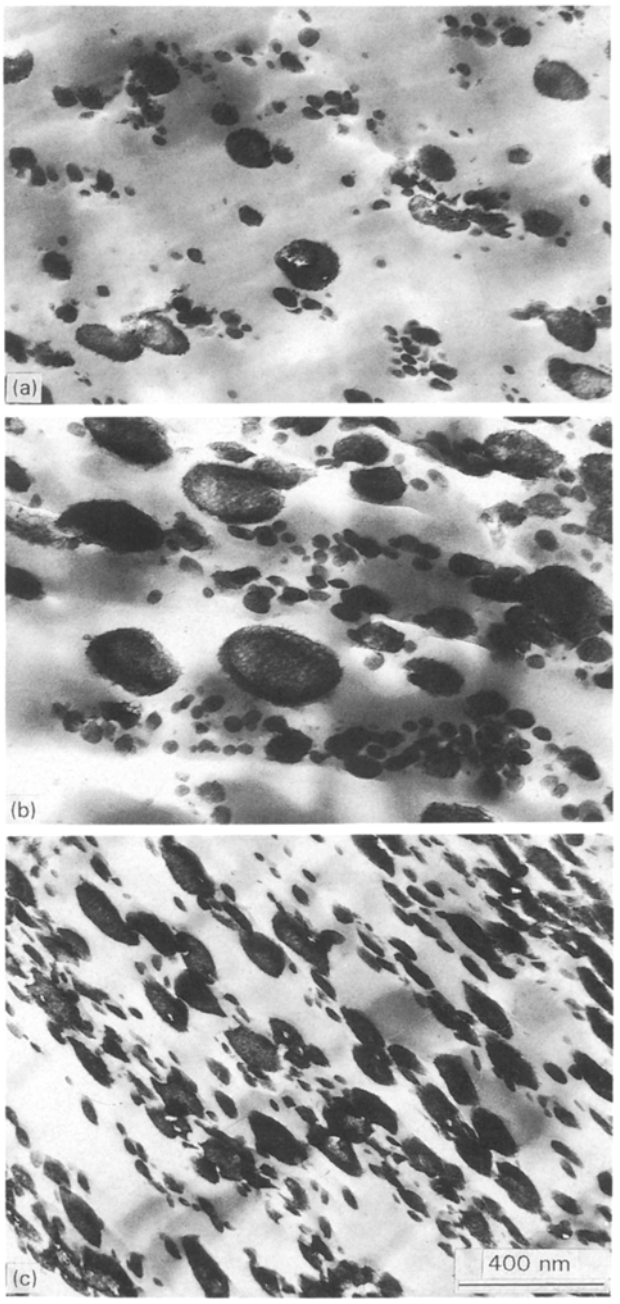

Figure 11 TEM observation of (a) T 85 MN, (b) T 65 MN, and (c) T 45 MN.

TABLE II Results of the quantitative morphological analysis

Bay-blend	Average particle size (nm)	Frequent particle size (nm)	90% spheres (nm)	Maximum particle size (nm)
T45 MN	132	93	73–190	310
T65 MN	172	87	70–261	512
T85 MN	123	73	57–182	370

An energy balance on the crack is the basis for a model [17] which includes energy dissipative processes in the evaluation of stable crack growth. According to this model, stable crack growth occurs if the energy dissipated in a material-specific way compensates for the surplus of available energy caused by crack propagation. Consequently, stable crack growth is controlled by the product JT_J.

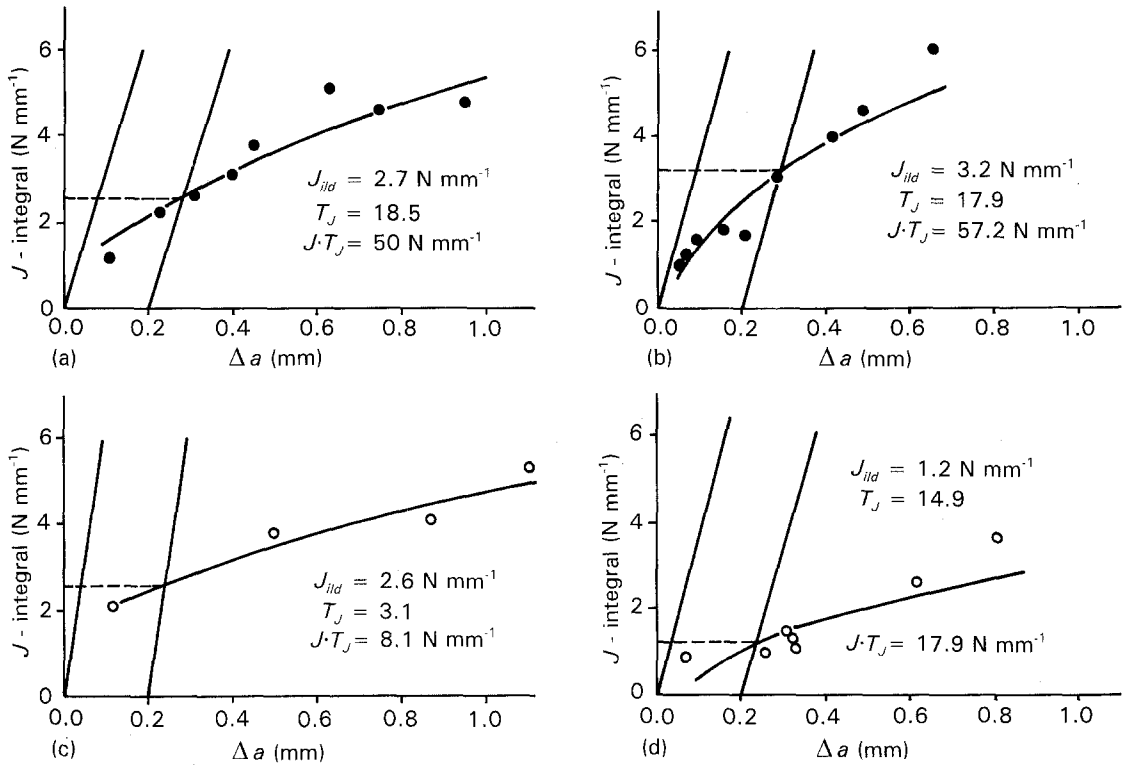

Figure 12 J versus Δa curves of (a, c) T 45 MN and (b, d) T 85 MN, evaluated with the JT_J concept. (a, b) RT, (c, d) $-30\,^{\circ}C$.

A physical concept is thus compared with an enlarged empirical description of toughness behaviour with the standards [10–12]. The expressiveness of this concept is shown below. If crack growth is controlled by the product JT_J, the J–Δa values must comply with Equation 6

$$J = (C_1 + C_2 \Delta a)^{\frac{1}{2}} \quad (6)$$

Fig. 12 shows the J versus Δa curves of T 45 MN and T 85 MN at room temperature and at $T = -30\,^{\circ}C$. The curve fitting is done using Equation 6. An evaluation of these J_R curves shows that the J_{ild} values of T 45 MN are the same for both temperatures. This means that the aim of obtaining high toughness properties at low temperatures is achieved. The influence of the test temperature becomes clear when the T_J values are increased with increasing temperature, and the product JT_J, which describes the energy absorption capacity of the material, is therefore also increased. T 85 MN exhibits an increase in the J_{ild} and T_J values with increasing temperature. The energy absorption capacity of T 85 MN is better than that of T 45 MN, especially at $T = -30\,^{\circ}C$. The morphological reason for this behaviour has already been discussed.

4. Conclusion

The investigations of PC/ABS blends with different ABS contents demonstrate that a combination of fracture mechanical investigation methods and an electron microscopical analysis of morphology and fracture surface structures makes it possible to obtain insight into materials behaviour. The continuation of such investigations should allow a purposeful toughness optimization at impact loading and/or low temperatures to be made on the basis of quantitative morphology–toughness correlations, as well as an energetical interpretation of fracture behaviour.

Acknowledgements

The authors thank Dr Oberbach and Dr. Schmachtenberg, Bayer AG Leverkusen, for the provision of all materials used in the experiments, and for helpful discussions.

References

1. J. G. WILLIAMS, "Fracture of Non-Metallic Materials" (1987) pp. 227–55.
2. I. NARISAWA and M. T. TAKEMORI, *Polym. Eng. Sci.* **29**, (1989) 671.
3. S. HASHEMI and J. G. WILLIAMS, *ibid.* **26** (1986) 760.
4. W. GRELLMANN, S. SEIDLER and J. BOHSE, *Kunststoffe* **81** (1991) 157.
5. W. GRELLMANN, S. SEIDLER and E. NEZBEDOVA, *Makromol. Chem. Macromol. Symp.* **41** (1991) 195.
6. W. GRELLMANN, S. SEIDLER, *J. Polym. Eng.*, **11** (1991) 71.
7. J. G. D. SUMPTER and C. E. TURNER, ASTM STP 601, 3 (American Society for Testing and Materials, Philadelphia, PA, 1976).
8. ASTM E 1152-87 (American Society for Testing and Materials, Philadelphia, PA, 1987).
9. U. ZERBST and P. WILL, *Neue Hüttte* **33** (1988) 269.
10. ASTM 813-89 (American Society for Testing and Materials, Philadelphia, PA, 1989).
11. DVM Merkblatt 002–87 (1987).
12. ESIS Procedure P2-91 (1991).
13. W. GRELLMANN and S. SEIDLER, *Materialprüfung* **33** (1991) 213.
14. A. SAVADORI, M. BRAMUZZO and C. MAREGA, *Polym. Test.* **4** (1984) 73.
15. S. SEIDLER and W. GRELLMANN, *Fortschr. Ber. VDI VDI-Reihe 18*, **92** (1991), VDI-Verlag Dusseldorf.
16. S. Wu, *Polymer* **26** (1985) 1855.
17. P. WILL, *Fortschr. Ber. VDI VDI Reihe 18*, **56** (1988), VDI-Verlag Dusseldorf.

Received 6 March 1992
and accepted 15 January 1993